Nox1-Based NADPH Oxidase Is the Major Source of UVA-Induced Reactive Oxygen Species in Human Keratinocytes

Antonio Valencia[1] and Irene E. Kochevar[1]

UVA radiation is a major environmental stress on skin, causing acute and chronic photodamage. These responses are mediated by reactive oxygen species (ROS), although the cellular source of these ROS is unknown. We tested the hypotheses that UVA-induced activation of nicotinamide adenine dinucleotide phosphate (NADPH) oxidase is required for ROS generation in human keratinocytes (HK) and that these ROS initiate rapid prostaglandin E_2 (PGE_2) synthesis. Treatment of HK with a non-toxic dose of UVA rapidly increased NADPH oxidase activity and intracellular ROS, which were partially blocked by an inhibitor of NADPH oxidase and by a mitochondria-selective antioxidant. Depleting the Nox1 isoform of the catalytic subunit of NADPH oxidase using small interfering RNA (siRNA) blocked the UVA-induced ROS increase, indicating that ROS produced by mitochondria or other sources are downstream from Nox1. Nox1 siRNA also blocked UVA-initiated PGE_2 synthesis. The mechanism for activation of Nox1 is mediated by an increase in intracellular calcium. Ceramide, which has been proposed to mediate responses to UVA in HK, also activated NADPH oxidase. These results indicate that UVA activates Nox1-based NADPH oxidase to produce ROS that stimulate PGE_2 synthesis, and that Nox1 may be an appropriate target for agents designed to block UVA-induced skin injury.

Journal of Investigative Dermatology (2008) **128,** 214–222; doi:10.1038/sj.jid.5700960; published online 5 July 2007

INTRODUCTION

UVA radiation, 320–400 nm, comprises about 95% of the solar UV reaching the earth's surface and initiates multiple responses in skin. Chronic exposure to solar UVA contributes to deleterious effects including skin cancer, tumor promotion, immunosuppression, and photoaging (de Laat *et al.*, 1997; Krutmann, 2001; Bachelor and Bowden, 2004; Allanson *et al.*, 2006). The role of UVA in development of cutaneous melanoma is still being debated (Setlow *et al.*, 1993; De Fabo *et al.*, 2004; Wood *et al.*, 2006). Acute responses in normal skin to UVA include rapid erythema and immediate pigment darkening as well as delayed erythema and tanning. Certain photosensitivity conditions are also induced by UVA (Charman *et al.*, 1998). Beneficial effects of UVA exposure include treatments for cutaneous scleroderma and atopic dermatitis (Krutmann, 2000; Breuckmann *et al.*, 2004).

Early studies established that UVA-induced erythema and tanning required oxygen in human skin (Auletta *et al.*, 1986) and more recent studies have clearly shown that responses in skin cells to UVA are mediated by reactive oxygen species (ROS). These ROS initiate signal transduction processes leading to rapid synthesis and release of inflammatory mediators, for example, prostaglandin E_2 (PGE_2) and isoprostanes, as well as induction of new gene products, for example, heme oxygenase-1, cytokines, cyclooxygenase, ICAM-1 (Grether-Beck *et al.*, 1996, 2005; Mahns *et al.*, 2004; Belli *et al.*, 2005). Despite their fundamental involvement in UVA-induced effects in skin, the types of the ROS responsible for initiating these responses are still unclear. The involvement of singlet oxygen ($^1O_2$) in UVA-induced responses is supported by studies showing enhanced responses in D_2O-containing media, which prolongs the lifetime $^1O_2$ but not the lifetimes of other ROS (Grether-Beck *et al.*, 1996; Tyrrell, 2000). Singlet oxygen is formed in cells by energy transfer to molecular oxygen from the triplet excited state of endogeneous chromophores possibly including porphyrins, NAD(P)H, flavins, cytochromes, heme, and other enzyme cofactors. Additional types of ROS are required for UVA-induced responses because $^1O_2$ is present only during the irradiation due to its short lifetime in cells (Skovsen *et al.*, 2005; Redmond and Kochevar, 2006) and ROS are detected long after the end of the UVA treatment. Thus, ROS continue to be produced for an extended period and, as ROS quenchers that do not affect $^1O_2$ block the responses, the ROS produced subsequent to $^1O_2$ appear to be required

[1]*Wellman Center for Photomedicine, Massachusetts General Hospital, Harvard Medical School, Boston, Massachusetts, USA*

Correspondence: Dr Irene E. Kochevar, Wellman Center for Photomedicine, Massachusetts General Hospital, Thier-224, 55 Fruit Street, Boston, MA 02114, USA. E-mail: kochevar@helix.mgh.harvard.edu

Abbreviations: BAPTA-AM, 1,2-bis-(O-aminophenoxy)-ethane-N,N,N′,N′-tetraacetic acid, tetraacetoxymethyl ester; $[Ca^{2+}]_i$, intracellular calcium concentration; carboxy-H_2DCFDA, 5-(and-6)-carboxy-2′,7′-dichlorodihydrofluorescein diacetate; DPI, diphenylene iodinium; HK, human keratinocytes; MitoQ or MQ, mitochondrially-targeted ubiquinone; PGE_2, prostaglandin E_2; ROS, reactive oxygen species

Received 24 January 2007; revised 23 March 2007; accepted 29 April 2007; published online 5 July 2007

for UVA-induced responses (Valencia *et al.*, 2006). The extended production of ROS after photosensitization to produce $^1O_2$ with an exogeneous dye has been demonstrated (Ouedraogo and Redmond, 2003). Potential cellular sources of extended production and enhanced levels of ROS include enzymes such as nicotinamide adenine dinucleotide phosphate (NADPH) oxidase, the mitochondrial electron transport chain and oxidation products from the reaction of $^1O_2$ with unsaturated lipids and proteins.

NADPH oxidase catalyzes the one-electron reduction of O_2 to superoxide anion (O_2^-) using NADPH as an electron donor. This enzymatic complex has been extensively studied in neutrophils and consists of plasma membrane-bound subunits ($gp91^{phox}$/Nox2 and $p22^{phox}$) and cytosolic subunits ($p40^{phox}$, $p47^{phox}$, $p67^{phox}$, Rac1) that assemble to produce the active enzyme (Babior *et al.*, 2002). Recently, homologues of these subunits have been described in several cell types and their activities investigated (Lambeth, 2004). Human keratinocytes (HK) express the $gp91^{phox}$/Nox2 catalytic subunit as well as its homologue, Nox1 (Chamulitrat *et al.*, 2004; He *et al.*, 2005; Valencia *et al.*, 2006). Murine keratinocytes express Nox2, although this subunit was shown to be only minimally involved in UVA-induced apoptosis (He *et al.*, 2005). We have recently shown that UVA irradiation of keratinocytes that are treated to have a high membrane content of 7-dehydrocholesterol (mimicking the UVA photosensitivity disease Smith–Lemli–Optiz syndrome) produce higher levels of ROS and that NADPH oxidase is involved in ROS generation (Valencia *et al.*, 2006). Whether UVA activates NADPH oxidase in normal keratinocytes has not been examined.

Previous studies have shown that UVA-initiated production of ROS involve mitochondria, as blocking complex I of the electron transport chain in the inner mitochondrial membrane inhibited ROS formation (Gniadecki *et al.*, 2000). In addition, UVA has been shown to cause lipid peroxidation in cell membranes (Morliere *et al.*, 1991), suggesting that ROS produced by chain radical oxidation of unsaturated lipids may also contribute to the extended formation of ROS after UVA.

In this study, we tested the hypotheses that the UVA-induced ROS formation in normal HK require the activation of the Nox1 catalytic subunit of NADPH oxidase and that these ROS stimulate synthesis of PGE_2 that can contribute to immediate and chronic UVA-induced skin responses.

RESULTS

NADPH oxidase is a major source of UVA-induced ROS in keratinocytes

Our previous results indicated that 10 J/cm^2 UVA was not cytotoxic to the same HK as used in this study (Valencia and Kochevar, 2006). In this study, HK were irradiated with 5 J/cm^2 and the relative level of intracellular ROS was quantified as a function of time after irradiation by measuring the fluorescence from the oxidation product of 5-(and-6)-carboxy-2′,7′-dichlorodihydrofluorescein diacetate (carboxy-H_2DCFDA) (Figure 1). A significant increase in ROS occurred by 5 minutes after irradiation in irradiated HK compared with non-irradiated controls. A maximum level of ROS was

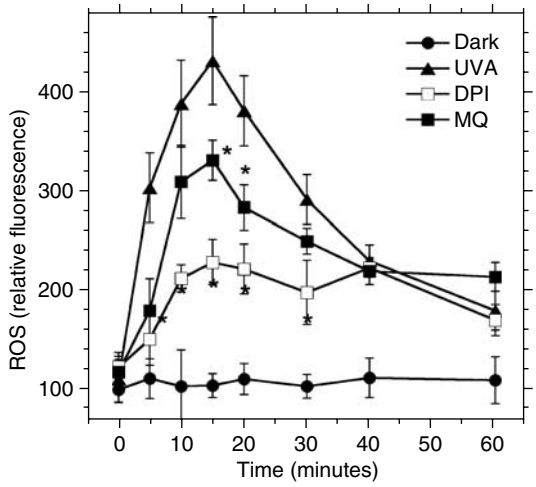

Figure 1. UVA induces rapid formation of ROS in keratinocytes that is partially quenched by an inhibitor of NADPH oxidase and a mitochondria-selective antioxidant. Keratinocytes were exposed to 5 J/cm^2 and the ROS level determined at varying times by measuring the fluorescence of the oxidation product of carboxy H_2DCFDA. UVA-irradiated HK were preincubated with DPI (1 μM), a NADPH oxidase inhibitor, or MitoQ, (0.1 μM), a mitochondria-selective antioxidant. The ROS level is shown as a function of time after UVA irradiation for non-irradiated HK (●), UVA-irradiated HK (▲), plus DPI (□), and plus MQ (■). Data are representative of four independent experiments with triplicate samples. *$P<0.01$ compared with UVA-irradiated HK at the same post-UVA time.

observed at 15 minutes and by 60 minutes the ROS level was only slightly greater than that in the unirradiated cells. Diphenylene iodinium (DPI) is often used as an inhibitor of NADPH oxidase, although it may not be entirely specific for this enzyme (Riganti *et al.*, 2004). DPI (1 μM) inhibited the UVA-induced level of ROS at 15 minutes by ~65%. As mitochondria are a potential source of ROS after UVA irradiation (Gniadecki *et al.*, 2000), we used mitochondrially-targeted ubiquinone (MitoQ or MQ), a recycling ubiquinone antioxidant that selectively localizes in mitochondria due to its triphenylphosphonium cation group, although a portion of the MitoQ taken up by cells localizes in non-mitochondrial membranes (Kelso *et al.*, 2001). The UVA-induced ROS level at 15 minutes was decreased by ~30% by 0.1 μM MitoQ, suggesting that ROS arising in mitochondria, and possibly other subcellular membranes, contribute to the ROS observed after UVA treatment, although at a lower level than NADPH oxidase. Neither DPI nor MitoQ alone completely decreased the ROS to that of the unirradiated control. Combining 0.1 μM MitoQ with 1 μM DPI did not produce a greater effect on UVA-induced ROS formation than the 65% reduction observed by DPI alone (results not shown). Higher levels of both agents were also tested (up to 5 μM of MitoQ plus 10 μM of DPI) in order to reduce the ROS level to baseline. However, these combinations resulted in cell death at 6 hours after UVA treatment (results not shown).

As DPI substantially decreased the UVA-induced ROS, the activity of NADPH oxidase was measured in HK as a function of time after UVA treatment. NADPH oxidase, measured as the superoxide dismutase-inhibitable cytochrome *c* oxidation

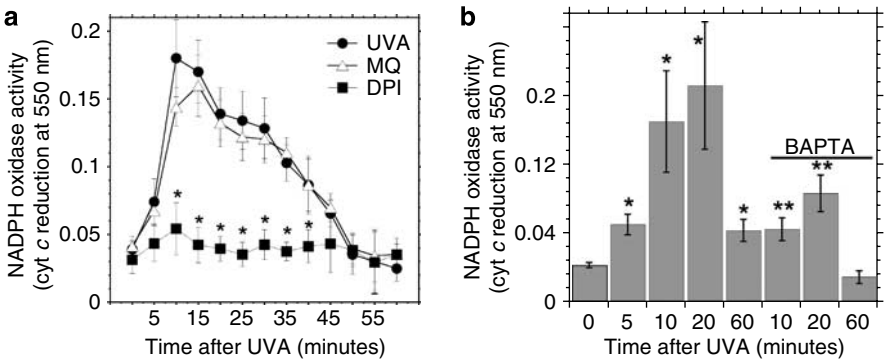

Figure 2. UVA increases NADPH oxidase activity of keratinocytes. Keratinocytes were exposed to 5 J/cm^2 UVA. (**a**) NADPH oxidase activity was measured as the cytochrome *c* oxidation at 550 nm in lysates from UVA-irradiated HK (●), plus DPI (■), or MQ (△) treatments. The ''zero time'' point represents cells before treatment. *$P<0.01$ compared with non-irradiated HK. Data are representative of five independent experiments with triplicate samples. (**b**) Keratinocytes were incubated for 60 minutes with the intracellular calcium chelator 25 μM BAPTA-AM before UVA treatment. *$P<0.01$ compared with non-irradiated HK. Data represent the average of four experiments with duplicate samples.

in membrane fractions obtained from cell lysates, was rapidly activated by UVA with a maximum activity at 10 minutes (Figure 2a). The activity gradually decreased to the level in unirradiated control cells at 60 minutes after UVA irradiation. The kinetics of UVA-induced NADPH oxidase activity is similar to those for ROS formation (Figure 1).

We tested the hypothesis that Nox1, one of the NADPH oxidase catalytic subunits expressed in HK, is the principal source of ROS formed in HK after UVA irradiation. RNA interference was used to knock down the levels Nox1. Two small interfering RNA (siRNA) (Nox1A-siRNA and Nox1B-siRNA) drastically decreased of ROS in UVA-irradiated HK, with nearly complete 100% inhibition of ROS production at 10, 15, and 20 minutes after UVA (Figure 3a). HK treated with scrambled sequence siRNA produced ROS levels after UVA identical to untreated HK. To assess the extent of that siRNA treatments reduced Nox1 protein, Western blotting was used. Levels of Nox1 using Nox1A-siRNA and Nox1B-siRNA were decreased in 90 and 85%, respectively, and scrambled siRNA did not affect the Nox1 level (Figure 3b). Blocking Nox1 protein synthesis by two different siRNA sequences strongly suggests that the observed inhibition of UVA-induced ROS is a Nox1-specific effect rather than a nonspecific effect of the siRNA treatment. The results in Figure 3a also show that Nox1 siRNA reduced the UVA-induced ROS most effectively at shorter times, as by 40 minutes the same ROS level was present in both siRNA-treated and -untreated samples, suggesting another source of ROS at longer times.

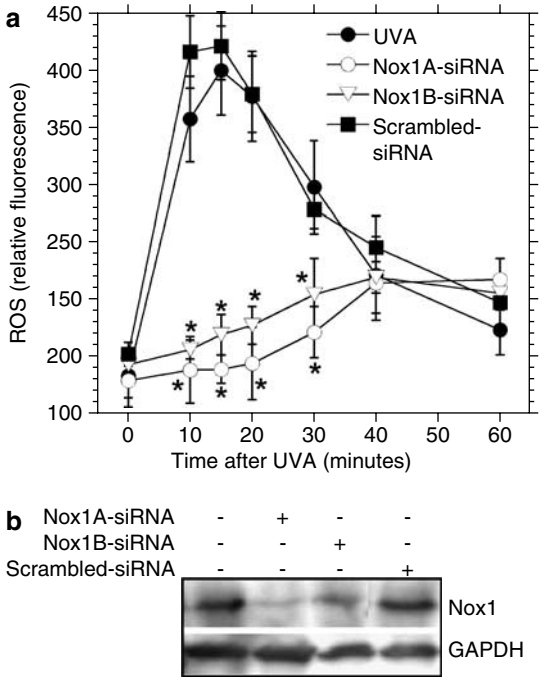

Figure 3. UVA-induced ROS formation in keratinocytes is inhibited in siRNA against Nox1. Keratinocytes were pretreated with two different siRNA sequences (Nox1A and Nox1B) against Nox1 of human NADPH oxidase or a scrambled sequence. (**a**) Kinetics of ROS formation in HK treated with Nox1A (○) or Nox1B (▽) siRNAs, a scrambled sequence (■) or buffer only (●) after irradiation with 5 J/cm^2 UVA. ROS level was measured using carboxy H_2DCFDA. *$P<0.01$ compared with UVA-irradiated HK not treated with Nox1 siRNA at the same post-UVA time. The ''zero time'' point represents cells before treatment. Data represent the average of four independent experiments with quadruplicate samples. (**b**) Nox1 levels were detected by Western blot in cells treated with Nox1A and Nox1B siRNA. Scrambled RNA was used as negative control. GAPDH levels are show as loading controls.

UVA increases Nox1-dependent PGE_2 release in HK

As UVA provokes a rapid increase in PGE_2 levels in skin, we monitored the release of PGE_2 as a function of time from UVA irradiated HK. PGE_2 release was significantly increased by 10 minutes after UVA, reached a maximum after 30–35 minutes, decreased and then reached another maximum after 120 minutes (Figure 4a). The PGE_2 level remained greater than the unirradiated control HK for at least 4 hours after UVA irradiation. The UVA-induced increase in PGE_2 release was blocked ~70%, compared to non-irradiated HK, by treatment with siRNA (Nox1A and Nox1B) at an early time (10 minutes), at the second maxima (120 minutes), and at the valley in between the maxima (60 minutes) (Figure 4b). However, DPI was only ~40% effective at reducing UVA-induced PGE_2 released at 60 and 120 minutes. Scrambled siRNA did not show any effect.

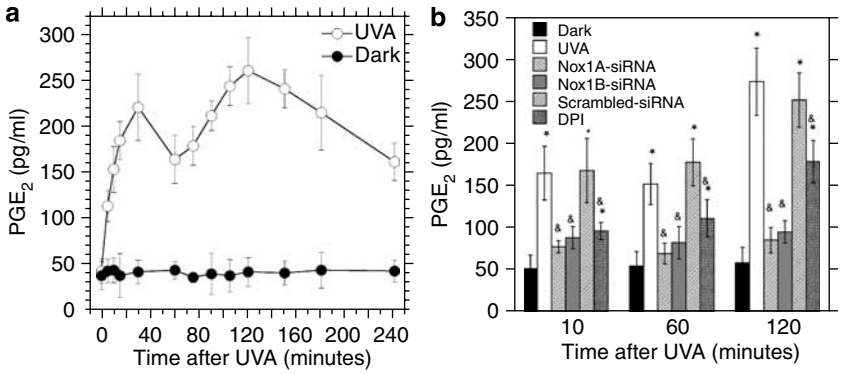

Figure 4. UVA induces PGE_2 release, which depends on Nox1 protein. Keratinocytes were treated with 5 J/cm^2. (**a**) Kinetics of rapid PGE_2 release measured by ELISA in UVA-irradiated HK (○) showing maxima at 30 and 120 minutes after UVA. Non-irradiated HK PGE_2 release is shown as filled circles (●). (**b**) Effects on PGE_2 release of inhibiting NADPH oxidase using DPI and Nox1 siRNA. Scrambled siRNA was used as negative control. $^{*,\ \&}P<0.01$ compared with non-irradiated HK and with UVA-irradiated HK, respectively, at the same time after UVA. Data represent the average of four independent experiments with quadruplicate samples.

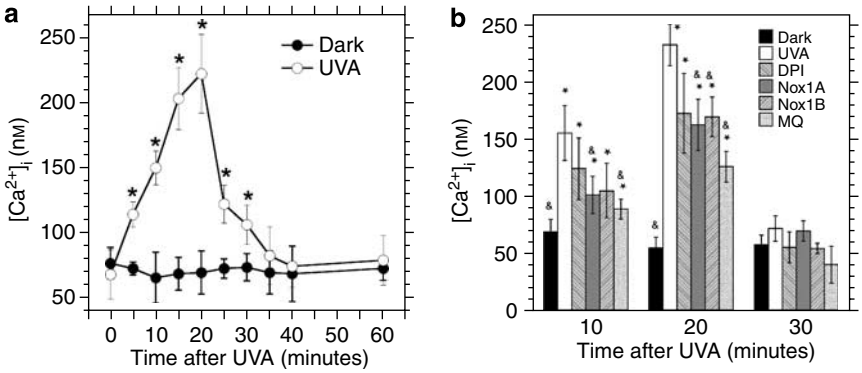

Figure 5. Intracellular calcium levels in keratinocytes increased rapidly after UVA and are blocked by Nox1 siRNA and an antioxidant. Keratinocytes were irradiated with 5 J/cm^2 UVA. (**a**) Kinetics of intracellular calcium levels measured by the fluorescence of Calcium Orange in unirradiated HK (●) and UVA-irradiated HK (○). $^*P<0.01$ compared with non-irradiated HK. The ''zero time'' point represents cells before treatment. Data represent the average of four independent experiments with triplicate samples. (**b**) Inhibition of UVA-induced intracellular calcium levels by the NADPH oxidase inhibitor DPI (1 μM), the mitochondria-selective antioxidant MitoQ (0.1 μM), and by depleting Nox1 using two siRNA. MitoQ and DPI were added 1 hour before UVA light in Hank's balanced salt solution. RNAi treatment was carried out 48 hours before irradiation. $^{*,\ \&}P<0.01$ compared with non-irradiated HK and UVA-irradiated HK at each time point, respectively. Data represent the average of three independent experiments with triplicate samples.

UVA-induced increase in intracellular calcium

UVA has been shown to increase intracellular calcium, $[Ca^{2+}]_i$, in fibroblasts (Maziere *et al.*, 2005). We measured the effect of pretreatment of HK with the calcium chelator 1,2-bis-(O-aminophenoxy)-ethane-N,N,N′,N′-tetraacetic acid, tetraacetoxymethyl ester (BAPTA-AM) (25 μM) on the UVA-induced activity of NADPH oxidase. As shown in Figure 2b, BAPTA-AM decreased NADPH oxidase by >70%. Next, we evaluated whether UVA induced an increase in $[Ca^{2+}]_i$ using the calcium-sensitive fluorescent probe Calcium Orange. $[Ca^{2+}]_i$ increased rapidly after UVA with a significant increase by 5 minutes and a maximum at 15–20 minutes (Figure 5a). The $[Ca^{2+}]_i$ decreased rapidly between 20 and 25 minutes and returned to basal concentrations by 35 minutes. In order to determine whether this spike in $[Ca^{2+}]_i$ resulted from ROS formation, and in particular by activation of NADPH oxidase, HK were treated with DPI or Nox1 siRNA or MQ before UVA treatment. DPI and siRNA (Nox1A and Nox1B) inhibited the UVA-induced increase in $[Ca^{2+}]_i$ at its maximum (20 minutes) by ~40% (Figure 5b). Interestingly, MQ was more effective than the NADPH oxidase inhibitors, reducing the $[Ca^{2+}]_i$ by ~55% at 20 minutes (Figure 4b). Measurements made at an earlier time (10 minutes after UVA) gave similar results except that Nox1 siRNA and MQ were more effective than at 20 minutes, reducing $[Ca^{2+}]_i$ by 60 and 75%, respectively.

Ceramide increases ROS production via NADPH oxidase activation

Ceramides have been shown to enhance ROS levels and activate NADPH oxidase in diverse cell types (Li *et al.*, 2002; Zhang *et al.*, 2003). In addition, UVA irradiation is reported to induce ceramide production in keratinocytes (Maziere *et al.*, 2001; Grether-Beck *et al.*, 2005). Consequently, we

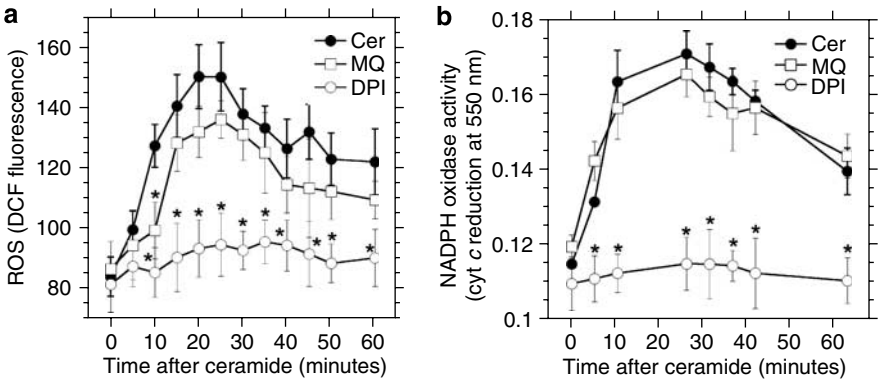

Figure 6. Ceramide induces rapid ROS formation in keratinocytes by activating NADPH oxidase. (**a**) Keratinocytes were treated with 25 μM C6 ceramide (●) plus 1 μM DPI (○) or plus 0.1 μM MQ (□). ROS levels were measured with carboxy H_2DCFDA. *$P<0.01$ compared with untreated HK. (**b**) NADPH oxidase activation measured as cytochrome *c* oxidation at 550 nm in HK lysates. Cells were lysed at varying times after addition of 25 μM C6 ceramide. Addition of 1 μM DPI (○) or 0.1 μM MQ (□) was carried out 1 hour before C6 ceramide treatment. *$P<0.001$ compared with untreated cells. Data represent the average of four independent experiments with triplicate samples.

examined whether ceramide might initiate ROS formation through the activation of NADPH oxidase in HK. Unirradiated HK were treated with C6-ceramide (25 μM) and the ROS formation was measured as a function of time. The ROS level rapidly increased reaching a maximum at 20–25 minutes (Figure 6a), similar to the kinetics for ROS after UVA treatment (Figure 1a). A single addition of C6-ceramide induced a sustained high level of ROS for 1 hour that returned to basal levels after 2 hours (data not shown). The NADPH oxidase activity was then measured over the same time course and showed similar kinetics than ROS production (Figure 6b). DPI inhibited the ceramide-induced increase in ROS nearly completely (Figure 6a) and blocked the increase in NADPH oxidase activity completely (Figure 6b). In contrast, MitoQ did not significantly alter the ROS or NADPH oxidase level induced by C6-ceramide, suggesting that mitochondrial or other sources of ROS downstream from NADPH oxidase do not participate in the ceramide-induced responses. In toto, these results suggest that ceramide might mediate the UVA-induced increase in NADPH.

DISCUSSION

Although UVA irradiation of cells is known to produce ROS, the intracellular sources of these reactive species are not well characterized and several phases of ROS production may occur. Multiple ROS including $^1O_2$, O_2^-, NO, H_2O_2, and lipid hydroperoxides have been detected or implicated in UVA-initiated responses (Tyrrell and Pidoux, 1989; Morliere *et al.*, 1991; Petersen *et al.*, 2000; Paunel *et al.*, 2005). Singlet oxygen is generally proposed to be the first ROS formed from triplet excited states of endogenous photosensitizers because replacing H_2O with D_2O increases certain UVA-induced responses, consistent with the longer lifetime of $^1O_2$, but not other ROS, in D_2O (Grether-Beck *et al.*, 1996; Tyrrell, 2000). Singlet oxygen, as well as O_2^- that may be formed by electron transfer from the excited state of the photosensitizer, is only present during the irradiation because of their short lifetimes in cells (Skovsen *et al.*, 2005; Redmond and Kochevar, 2006). However, these initial species must induce extended production of additional ROS, as ROS are detected for an extended period after UVA exposure (Figure 1) (Valencia *et al.*, 2006).

In this study, we focused on NADPH oxidase and mitochondria as sources for extended ROS production after UVA irradiation and tested whether these ROS are responsible for a rapid response of keratinocytes, namely, the production of PGE_2. Our initial results using small molecule inhibitors with different selectivities, DPI and MitoQ, indicated that ROS are produced by more than one mechanism, as both inhibitors only partially blocked ROS formation (Figure 1). In addition, the time course for UVA-induced NADPH oxidase activity paralleled that for ROS formation (Figure 2a), suggesting that this redox active enzyme was involved. These results did not allow us to discriminate between concurrent production of ROS from different subcellular sources and sequential generation of ROS from different sources. However, when Nox1 protein was 85–95% depleted, the UVA-induced ROS level was decreased by comparable amounts (Figure 3a) indicating that the production of ROS after UVA requires Nox1 activity and implying that Nox1 activity is upstream of ROS production by mitochondria and other cellular sources. A similar sequence for ROS formation was found during rat cardiac ischemia/reperfusion injury where angiotensin II-induced activation of NADPH oxidase led to production of a much larger amount of ROS by mitochondria (Kimura *et al.*, 2005). Mitochondrial ROS can also elicit ROS formation by NADPH oxidase, as serum withdrawal that stimulated production of ROS by mitochondria subsequently, by a phosphatidylinositol 3-kinase-dependent mechanism, induced ROS production by NADPH oxidase (Lee *et al.*, 2006). These are all examples of the more general phenomenon of ROS-induced ROS formation (Zorov *et al.*, 2000; Kimura *et al.*, 2005).

The mechanism by which the O_2^- produced by Nox1 elicits further ROS formation in cells may follow more than one pathway. Nox1 is localized in the plasma membrane in most cell types and releases O_2^- to the extracellular space (Lambeth, 2004; Takeya and Sumimoto, 2006). Dismutation

of O_2^- outside of cells forms H_2O_2 that can diffuse into the same cell, or nearby cells, to elicit responses. Extracellular catalase blocks NADPH oxidase-mediated responses verifying the extracellular formation of H_2O_2 (Liu *et al.*, 2006). Exogenous H_2O_2 has also been shown to increase intracellular ROS from endogenous sources (Li *et al.*, 2001; Chernyak *et al.*, 2006). An alternative pathway involves products of membrane lipid peroxidation, such as 4-hydroxynonenal, that have been shown to stimulate ROS formation by mitochondria (Landar *et al.*, 2006). Mitochondria are not necessarily the source of ROS after activation of Nox1. Although MitoQ is concentrated in mitochondria, it also partially distributes to other cell membranes and, consequently, may block lipid peroxidation at non-mitochondrial sites (Kelso *et al.*, 2001; James *et al.*, 2005). MitoQ acts as a membrane-localized antioxidant with the ubiquinol portion of the MitoQ structure buried in the lipid bilayer where it reacts with hydroperoxy or lipid peroxy radicals to terminate lipid oxidation chain reactions (Kelso *et al.*, 2001; James *et al.*, 2005). Overall, our results indicate that the primary site for the extended production of ROS after UVA treatment is the Nox1-containing isoform of NADPH oxidase in keratinocytes and that mitochondria, as well as other membranes, may also supply downstream ROS.

The mechanism for activation of Nox1 by UVA irradiation is unknown. Activation of Nox1 requires activation of Rac1 and its translocation to the plasma membrane where it binds to the preassembled complex of Nox1, NoxO1 (''Nox organizer''), and NoxA1 (''Nox activator'') (Park *et al.*, 2004; Ueyama *et al.*, 2006). Our results suggest two possible mechanisms for the activation of Rac1 by the $^1O_2$ formed during UVA irradiation. In one mechanism, $^1O_2$ causes an increase in $[Ca^{2+}]_i$, as shown previously for photosensitization (Kessel *et al.*, 2005), which leads to activation of NADPH oxidase (Figure 2b). Nox1 itself is not directly calcium dependent (Lambeth, 2004) but, an increase $[Ca^{2+}]_i$ has been shown to activate Rac (Mehta *et al.*, 2005). Based on studies in prostate carcinoma cells, the mechanism may involve activation of protein kinase C by Ca^{2+}, subsequent phosphorylation of the Rac inhibitor RhoGDIα, which allows Rac to translocate to the plasma membrane (Price *et al.*, 2003). Interestingly, the UVA-induced increase in the $[Ca^{2+}]_i$ level (Figure 5b) was partially inhibited (~35%) by Nox1 siRNA, suggesting a positive feedback process: UVA increases $[Ca^{2+}]_i$, which activates Nox1 thereby increasing the ROS that stimulate a further increase in $[Ca]_i$. Our studies do not define the source of increased $[Ca^{2+}]_i$, although the UVA-induced increase is partially blocked (~55%) by MitoQ suggesting Ca^{2+} release from mitochondria. An alternative mechanism for activation of Rac1 by $^1O_2$ relies on the rapid release of ceramide after UVA, which has been investigated in keratinocytes (Maziere *et al.*, 2001; Grether-Beck *et al.*, 2005). Ceramide has been shown to activate Rac1 leading to ROS formation by NADPH oxidase in rat mesangial cells (Yi *et al.*, 2004). The mechanism for this process has not been established in keratinocytes but may involve ceramide-induced activation of phosphatidylinositol 3-kinase (Barsacchi *et al.*, 2003), which is a known activator of Rac1 via the guanine nucleotide exchange factor β-Pix (Park *et al.*, 2004).

The ROS produced by NADPH oxidase are responsible for the UVA-initiated increase in PGE_2, as depletion of Nox1 protein using siRNA nearly completely blocked this response at both the first (10 minutes) and second maxima (120 minutes) (Figure 4b). Interestingly, Nox1 siRNA treatment only blocked ROS formation up to 30 minutes post-irradiation (Figure 3a), suggesting that even the PGE_2 contributing to the maximum at 120 minutes requires Nox1 activity at much shorter times after UVA (<30 minutes). The ROS produced in a Nox1-independent manner at times >30 minutes post-UVA does not appear to influence PGE_2 synthesis. The rapid kinetics of the PGE_2 increase (Figure 4a) correlates with those for the $[Ca^{2+}]_i$ increase (Figure 5a). These two species are linked by the fact that cytosolic PLA_2, which cleaves arachidonic acid from membrane phospholipids leading to PGE_2 synthesis, is activated by Ca^{2+}.

In summary, UVA treatment stimulates formation of ROS in keratinocytes via a Nox1-based NADPH oxidase. Our results suggest that the mechanism for activation of Nox1 involves UVA-induced increase in $[Ca^{2+}]_i$ and ceramide, presumably resulting from initial formation of $^1O_2$, that lead to activation of Rac1. The ROS formed initiate production of additional ROS from oxidation of mitochondrial and possibly other membranes and induce synthesis of PGE_2, an inflammatory mediator after UVA irradiation, by a Ca^{2+}-dependent mechanism. The role of these ROS in additional UVA-induced responses in keratinocytes requires further study. These results suggest that agents that inhibit the Nox1-containing isoform of NADPH oxidase might block UVA-induced skin injury. Such agents would need to be specific for Nox1 to prevent interfering with the activity and potentially beneficial effects of the phagocyte Nox2-containing isoform of this enzyme.

MATERIALS AND METHODS

Culture of HK

HK immortalized by expression of the catalytic subunit of telomerase were a gift from Dr James Rheinwald (NIH Harvard Skin Disease Research Center). Cells were plated in serum-free keratinocyte medium with phenol red (Gibco Invitrogen, Carlsbad, CA) supplemented with recombinant EGF (2.5 μg/500 ml from Gibco, Invitrogen), bovine pituitary extract (25 mg/500 ml, Gibco), 0.3 mM $CaCl_2$, 50 mg streptomycin, and 50,000 U of penicillin per 500 ml of media (Sigma, St Louis, MO). HK were incubated at 37°C, 5% CO_2 and medium was replaced every 48 hours until the cells reached 50–60% confluence.

UVA irradiation

The fluorescent UVA broadband lamps (320–420 nm, PUVA 180; Herbert Waldman, Werk für lichtechnik Schwenningen, Germany) used had an irradiance of 5.1 mW/cm^2. Cells were irradiated in Hank's balanced salt solution after removing the culture plate lids and the temperature remained ~32°C. Immediately after irradiation medium was replaced with fresh serum-free keratinocyte medium or the appropriate treatment medium.

Detection of ROS

Cells grown in 12- and 6-multiwell plates were incubated for 30 minutes at 37°C with 5 μM of carboxy-H_2DCFDA (Molecular Probes Inc., Molecular Probes Invitrogen, Carlsbad, CA) in Hank's balanced salt solution and irradiated with 5 J/cm^2 UVA (~15 minutes exposure). For ROS measurements at 60 minutes and longer times, carboxy-H_2DCFDA was added after UVA irradiation, keeping the incubation time at 30 minutes before measurements. After UVA irradiation, the fluorescence was detected using a dual scanning microplate spectrofluorometer (Spectra MAX Gemini EM, Molecular Devices, Sunnyvale, CA) with 480 nm excitation and 530 nm emission.

Preparation of cell fractions and NADPH oxidase activity assay

The isolation of cellular membranes and the NADPH oxidase activity measurements were carried out as described previously (Valencia and Kochevar, 2006). Briefly, cellular homogenates from 3×10^6 cells per sample were obtained in lysis buffer (eight parts of 150 mM K, Na phosphate buffer pH 7.4, 1 mM $MgCl_2$, 1 mM EGTA, 2 mM NaN_3, 1 mM dithiothreitol, and two parts of glycerol containing 50 mM octylglycoside). Post-nuclear fraction was discarded after centrifuged the lysate at 1000 r.p.m. for 10 minutes at 4°C. Supernatant was centrifuged at 25 000 r.p.m. in a Beckman Coulter Optima™ L-90K Ultracentrifuge using a NVT 90 rotor for 1 hour at 4°C. The pellet was recovered in resuspension buffer (65 mM K, Na phosphate buffer pH 7.4, 1 mM $MgCl_2$, 1 mM EGTA, 2 mM NaN_3, 1 mM dithiothreitol, 20 μg/ml leupeptin, 10 μg/ml pepstatin A, 10 μg/ml aprotinin, and 2 mM phenylmethylsulfonyl fluoride) and used as the membrane fraction. The supernatant was centrifuged at 65 000 r.p.m. using the NVT 90 rotor for 1 hour at 4°C. The supernatant cytosolic fraction was used for determination of NADPH oxidase activity. Protein content was determined by Bradford assay.

The superoxide dismutase-inhibitable activity of NADPH oxidase was determined by ferricytochrome *c* reduction in octylglycoside-containing buffer (Shpungin *et al.*, 1989). Twenty and sixty micrograms of protein, respectively, from membrane and cytosolic fractions were incubated in the reaction mixture (0.1 mM cytochrome *c*, 65 mM K, Na phosphate buffer pH 6.8, 2 mM EGTA, 1 mM $MgCl_2$, and 10 μM flavin adenosine dinucleotide) plus 100 μM of SDS for 2 minutes at 24°C. Then, superoxide anion production from NADPH oxidase complex was induced by addition of 0.2 mM of NADPH. The absorbance of reduced cytochrome *c* was measured at 550 nm using a spectrophotometer (Aglient 8453 UV-visible Spectroscopy System, Aglient Technologies, Foster City, CA). Results are expressed as absorbance of cytochrome *c* reduced at 550 nm.

Silencing Nox1 by RNA interference

Silencing Nox1 experiments were carried out following the protocol described in a previous study (Valencia and Kochevar, 2006). Stealth™-siRNA duplex oligoribonucleotides (Invitrogen™ Life Technologies, Carlsbad, CA) were designed by selecting two different duplex sequences of the human Nox1 gene, which is the catalytic subunit of a non-phagocytic NADPH oxidase expressed by keratinocytes (Chamulitrat *et al.*, 2004). Nox1-A primer with the sequence sense 5′-ACAAUAGCCUUGAUUCUCAUGGUAA-3′, anti-sense 5′-UUAC CAUGAGAAUCAAGGCUAUUGU-3′, starting at 750 bp; and Nox1-B primer with sequence sense 5′-GCAAUAUUG UUGGUCAUGCAG CAUU-3′, anti-sense 5′-AAUG CUGCAUGACCAACAAUAUUGC-3′, located at 1642 bp. A scrambled Stealth™ siRNA duplex as a negative control was used with sequence sense 5′-ACACCGAA GUUUCUUGUACGUAUAA-3′, anti-sense 5′-UUAUACGUACAA GAAACUUCGGUGU-3′. Transfection efficiency was determined with the Silencer^R FAM™ labeled negative control siRNA (Ambion, Austin, TX).

Optimal transfection efficiency by the amounts of transfection reagent (Lipofectamine-2000™ from Invitrogen™ Life Technologies), siRNA, cell density, and the length of exposure of cells to Lipofectmanie2000™-siRNA complexes were optimized in our previous study (Valencia and Kochevar, 2006). Briefly, at 24 hours before transfection, HK were transferred onto six-well plates (8×10^5 cells/well) and transfected with 100 nM of each Stealth™-siRNA duplex using Lipofectamine-2000™ transfection reagent for 4 hours in serum-reduced media (OptiMem from Gibco Invitrogen) without antibiotics. Then, complete serum-free keratinocyte medium was added to the HK. Maximum levels of transfection were observed at 48 hours with both Nox1-A and Nox1-B primers. Transfection efficiency was monitored by flow cytometry based on FAM-labeled transfected cells, resulted in 75% transfection efficiency with Nox1-A Stealth™-siRNA and 70% with Nox1-B Stealth™-siRNA. Cell death was measured by flow cytometry using 7-amino-actinomicyn D, an early apoptotic marker that intercalates in the DNA of apoptotic cells, resulting in 9 and 13% cell death for Nox1-A and Nox1-B, respectively.

Prostaglandin E_2 release

PGE_2 release was assayed using a commercial EIA kit (Cayman Chemical; Ann Arbor, MI). The PGE_2 release was detected by the absorption of 5-thio-2-nitrobenzoic acid at 412 nm, which is the product of non-enzymatic reaction between PGE_2-acetylcholinesterase and acetylthiolcholine plus 5-5′-dithio-bis-(2-nitrobenzoic acid). For these experiments, six-well plates were used containing ~400 000 cells at 80% confluence. Results are express as a picogram of PGE_2 released per cell.

Intracellular calcium levels

Intracellular calcium was measured using the fluorescent probe Calcium Orange™-AM from Molecular Probes Inc. Cells in six-well plates (~520 000 per sample) were incubated with 10 μM of Calcium Orange™-AM for 30 minutes at 37°C. Then the fluorescence was detected in a dual scanning microplate spectrofluorometer (Spectra MAX Gemini EM, Molecular Devices) using 530 nm excitation and 575 nm emission wavelengths. To obtain the total free $[Ca^{2+}]_i$ in the samples, the following formula was applied:

$$[Ca^{2+}]_i = K_d(F - F_{min}/F_{max} - F)$$

when K_d is the dissociation constant for Calcium Orange™ (185 nM), F is fluorescence of experimental samples, F_{min} is the fluorescence in the absence of calcium and F_{max} is the fluorescence of calcium-saturated probe. Calibration was carried out using ionomicyn (1 μM in DMSO; Molecular Probes Inc.) and BAPTA-AM (5 μM 1 hour preincubation; Molecular Probes Inc.).

Immunoblots

Cells homogenates were obtained in lysis buffer (250 mM Tris-HCl pH 6.8, 150 mM NaCl, 4% (w/v) SDS, 0.5 mM EGTA, 5 mM dithio-

threitol, 20 μg/ml leupeptin, 10 μg/ml pepstatin A, 10 μg/ml aprotinin, and 2 mM phenylmethylsulfonyl fluoride). Samples were subjected to SDS-PAGE and the resolved proteins were transferred to polyvinylidine difluoride membranes at 100 mV for 1 hour at 4°C. Membranes were blocked with 5% non-fat milk in Tris-buffered saline (phosphate-buffered saline plus 0.1% (v/v) Tween 20) for 1–2 hours. Primary antibodies were incubated in 2.5% non-fat milk in Tris-buffered saline overnight at 4°C followed by 1 hour incubation with hypoxanthine-guanine phosphoribosyl-transferase (HPRT)-linked secondary antibody. Bands were visualized using enhanced chemiluminescence system according to the manufacturer (Cell Signaling, Beverly MA). Anti-Nox1 antibody was from Santa Cruz Biotechnology Inc., Santa Cruz, CA.

Statistical analysis

Data are expressed as mean ± SD, and statistical significance of the results was determined by one-way analysis of variance followed by *t*-test, with statistical significance set at $P<0.01$.

CONFLICT OF INTEREST

The authors state no conflict of interest.

ACKNOWLEDGMENTS

We thank William Farinelli for technical support, Dr Michael P Murphy for kindly supplying the MitoQ, and Chelvi Rajadurai for helpful technical assistance. This research was supported by NIH Grant GM 30955 (IEK). AV was partially supported by the Fundacion Mexico en Harvard, AC.

REFERENCES

Allanson M, Domanski D, Reeve VE (2006) Photoimmunoprotection by UVA (320–400 nm) radiation is determined by UVA dose and is associated with cutaneous cyclic guanosine monophosphate. *J Invest Dermatol* 126:191–7

Auletta M, Gange RW, Tan OT, Matzinger E (1986) Effect of cutaneous hypoxia upon erythema and pigment responses to UVA, UVB, and PUVA (8-MOP+UVA) in human skin. *J Invest Dermatol* 86:649–52

Babior BM, Lambeth JD, Nauseef W (2002) The neutrophil NADPH oxidase. *Arch Biochem Biophys* 397:342–4

Bachelor MA, Bowden GT (2004) UVA-mediated activation of signaling pathways involved in skin tumor promotion and progression. *Semin Cancer Biol* 14:131–8

Barsacchi R, Perrotta C, Bulotta S, Moncada S, Borgese N, Clementi E (2003) Activation of endothelial nitric-oxide synthase by tumor necrosis factor-alpha: a novel pathway involving sequential activation of neutral sphingomyelinase, phosphatidylinositol-3′ kinase, and Akt. *Mol Pharmacol* 63:886–95

Belli R, Amerio P, Brunetti L, Orlando G, Toto P, Proietto G *et al.* (2005) Elevated 8-isoprostane levels in basal cell carcinoma and in UVA irradiated skin. *Int J Immunopathol Pharmacol* 18:497–502

Breuckmann F, Gambichler T, Altmeyer P, Kreuter A (2004) UVA/UVA1 phototherapy and PUVA photochemotherapy in connective tissue diseases and related disorders: a research based review. *BMC Dermatol* 4:11

Chamulitrat W, Stremmel W, Kawahara T, Rokutan K, Fujii H, Wingler K *et al.* (2004) A constitutive NADPH oxidase-like system containing gp91phox homologs in human keratinocytes. *J Invest Dermatol* 122:1000–9

Charman CR, Ryan A, Tyrrell RM, Pearse AD, Arlett CF, Kurwa HA *et al.* (1998) Photosensitivity associated with the Smith–Lemli–Opitz syndrome. *Br J Dermatol* 138:885–8

Chernyak BV, Izyumov DS, Lyamzaev KG, Pashkovskaya AA, Pletjushkina OY, Antonenko YN *et al.* (2006) Production of reactive oxygen species in mitochondria of HeLa cells under oxidative stress. *Biochim Biophys Acta* 1757:525–34

De Fabo EC, Noonan FP, Fears T, Merlino G (2004) Ultraviolet B but not ultraviolet A radiation initiates melanoma. *Cancer Res* 64:6372–6

de Laat A, van der Leun JC, de Gruijl FR (1997) Carcinogenesis induced by UVA (365-nm) radiation: the dose-time dependence of tumor formation in hairless mice. *Carcinogenesis* 18:1013–20

Gniadecki R, Thorn T, Vicanova J, Petersen A, Wulf HC (2000) Role of mitochondria in ultraviolet-induced oxidative stress. *J Cell Biochem* 80:216–22

Grether-Beck S, Olaizola-Horn S, Schmitt H, Grewe M, Jahnke A, Johnson JP *et al.* (1996) Activation of transcription factor AP-2 mediates UVA radiation- and singlet oxygen-induced expression of the human intercellular adhesion molecule 1 gene. *Proc Natl Acad Sci USA* 93:14586–91

Grether-Beck S, Timmer A, Felsner I, Brenden H, Brammertz D, Krutmann J (2005) Ultraviolet A-induced signaling involves a ceramide-mediated autocrine loop leading to ceramide *de novo* synthesis. *J Invest Dermatol* 125:545–53

He YY, Huang JL, Block ML, Hong JS, Chignell CF (2005) Role of phagocyte oxidase in UVA-induced oxidative stress and apoptosis in keratinocytes. *J Invest Dermatol* 125:560–6

James AM, Cocheme HM, Smith RA, Murphy MP (2005) Interactions of mitochondria-targeted and untargeted ubiquinones with the mitochondrial respiratory chain and reactive oxygen species. Implications for the use of exogenous ubiquinones as therapies and experimental tools. *J Biol Chem* 280:21295–312

Kelso GF, Porteous CM, Coulter CV, Hughes G, Porteous WK, Ledgerwood EC *et al.* (2001) Selective targeting of a redox-active ubiquinone to mitochondria within cells: antioxidant and antiapoptotic properties. *J Biol Chem* 276:4588–96

Kessel D, Castelli M, Reiners JJ (2005) Ruthenium red-mediated suppression of Bcl-2 loss and Ca(2+) release initiated by photodamage to the endoplasmic reticulum: scavenging of reactive oxygen species. *Cell Death Differ* 12:502–11

Kimura S, Zhang GX, Nishiyama A, Shokoji T, Yao L, Fan YY *et al.* (2005) Role of NAD(P)H oxidase- and mitochondria-derived reactive oxygen species in cardioprotection of ischemic reperfusion injury by angiotensin II. *Hypertension* 45:860–6

Krutmann J (2000) Phototherapy for atopic dermatitis. *Clin Exp Dermatol* 25:552–8

Krutmann J (2001) The role of UVA rays in skin aging. *Eur J Dermatol* 11:170–1

Lambeth JD (2004) NOX enzymes and the biology of reactive oxygen. *Nat Rev Immunol* 4:181–9

Landar A, Zmijewski JW, Dickinson DA, Le Goffe C, Johnson MS, Milne GL *et al.* (2006) Interaction of electrophilic lipid oxidation products with mitochondria in endothelial cells and formation of reactive oxygen species. *Am J Physiol Heart Circ Physiol* 290: H1777–87

Lee SB, Bae IH, Bae YS, Um HD (2006) Link between mitochondria and NADPH oxidase 1 isozyme for the sustained production of reactive oxygen species and cell death. *J Biol Chem* 281:36228–35

Li H, Junk P, Huwiler A, Burkhardt C, Wallerath T, Pfeilschifter J *et al.* (2002) Dual effect of ceramide on human endothelial cells: induction of oxidative stress and transcriptional upregulation of endothelial nitric oxide synthase. *Circulation* 106:2250–6

Li WG, Miller FJ Jr, Zhang HJ, Spitz DR, Oberley LW, Weintraub NL (2001) H(2)O(2)-induced O(2) production by a non-phagocytic NAD(P)H oxidase causes oxidant injury. *J Biol Chem* 276:29251–6

Liu Y, Hao W, Letiembre M, Walter S, Kulanga M, Neumann H *et al.* (2006) Suppression of microglial inflammatory activity by myelin phagocytosis: role of p47-PHOX-mediated generation of reactive oxygen species. *J Neurosci* 26:12904–13

Mahns A, Wolber R, Stab F, Klotz LO, Sies H (2004) Contribution of UVB and UVA to UV-dependent stimulation of cyclooxygenase-2 expression in artificial epidermis. *Photochem Photobiol Sci* 3:257–62

Maziere C, Conte MA, Leborgne L, Levade T, Hornebeck W, Santus R *et al.* (2001) UVA radiation stimulates ceramide production: relationship to oxidative stress and potential role in ERK, JNK, and p38 activation. *Biochem Biophys Res Commun* 281:289–94

Maziere C, Morliere P, Louandre C, Conte MA, Gomilla C, Santus R *et al.* (2005) Low UVA doses activate the transcription factor NFAT in human fibroblasts by a calcium-calcineurin pathway. *Free Radic Biol Med* 39:1629–37

Mehta D, Konstantoulaki M, Ahmmed GU, Malik AB (2005) Sphingosine 1-phosphate-induced mobilization of intracellular Ca2+ mediates rac activation and adherens junction assembly in endothelial cells. *J Biol Chem* 280:17320–8

Morliere P, Moysan A, Santus R, Huppe G, Maziere JC, Dubertret L (1991) UVA-induced lipid peroxidation in cultured human fibroblasts. *Biochim Biophys Acta* 1084:261–8

Ouedraogo GD, Redmond RW (2003) Secondary reactive oxygen species extend the range of photosensitization effects in cells: DNA damage produced via initial membrane photosensitization. *Photochem Photobiol* 77:192–203

Park HS, Lee SH, Park D, Lee JS, Ryu SH, Lee WJ *et al.* (2004) Sequential activation of phosphatidylinositol 3-kinase, beta Pix, Rac1, and Nox1 in growth factor-induced production of H2O2. *Mol Cell Biol* 24:4384–94

Paunel AN, Dejam A, Thelen S, Kirsch M, Horstjann M, Gharini P *et al.* (2005) Enzyme-independent nitric oxide formation during UVA challenge of human skin: characterization, molecular sources, and mechanisms. *Free Radic Biol Med* 38:606–15

Petersen AB, Gniadecki R, Vicanova J, Thorn T, Wulf HC (2000) Hydrogen peroxide is responsible for UVA-induced DNA damage measured by alkaline comet assay in HaCaT keratinocytes. *J Photochem Photobiol B* 59:123–31

Price LS, Langeslag M, ten Klooster JP, Hordijk PL, Jalink K, Collard JG (2003) Calcium signaling regulates translocation and activation of Rac. *J Biol Chem* 278:39413–21

Redmond RW, Kochevar IE (2006) Spatially-resolved cellular responses to singlet oxygen. *Photochem Photobiol* 82:1178–86

Riganti C, Gazzano E, Polimeni M, Costamagna C, Bosia A, Ghigo D (2004) Diphenyleneiodonium inhibits the cell redox metabolism and induces oxidative stress. *J Biol Chem* 279:47726–31

Setlow RB, Grist E, Thompson K, Woodhead AD (1993) Wavelengths effective in induction of malignant melanoma. *Proc Natl Acad Sci USA* 90:6666–70

Shpungin S, Dotan I, Abo A, Pick E (1989) Activation of the superoxide forming NADPH oxidase in a cell-free system by sodium dodecyl sulfate. Absolute lipid dependence of the solubilized enzyme. *J Biol Chem* 264:9195–203

Skovsen E, Snyder JW, Lambert JD, Ogilby PR (2005) Lifetime and diffusion of singlet oxygen in a cell. *J Phys Chem B Condens Matter Mater Surf Interfaces Biophys* 109:8570–3

Takeya R, Sumimoto H (2006) Regulation of novel superoxide-producing NAD(P)H oxidases. *Antioxid Redox Signal* 8:1523–32

Tyrrell RM (2000) Role for singlet oxygen in biological effects of ultraviolet A radiation. *Methods Enzymol* 319:290–6

Tyrrell RM, Pidoux M (1989) Singlet oxygen involvement in the inactivation of cultured human fibroblasts by UVA (334, 365 nm) and near-visible (405 nm) radiations. *Photochem Photobiol* 49:407–12

Ueyama T, Geiszt M, Leto TL (2006) Involvement of Rac1 in activation of multicomponent Nox1- and Nox3-based NADPH oxidases. *Mol Cell Biol* 26:2160–74

Valencia A, Kochevar IE (2006) Ultraviolet A induces apoptosis via reactive oxygen species in a model for Smith–Lemli–Opitz syndrome. *Free Radic Biol Med* 40:641–50

Valencia A, Rajadurai A, Carle AB, Kochevar IE (2006) 7-Dehydrocholesterol enhances ultraviolet A-induced oxidative stress in keratinocytes: Roles of NADPH oxidase, mitochondria and lipid rafts. *Free Radic Biol Med* 41:1704–18

Wood SR, Berwick M, Ley RD, Walter RB, Setlow RB, Timmins GS (2006) UV causation of melanoma in Xiphophorus is dominated by melanin photosensitized oxidant production. *Proc Natl Acad Sci USA* 103:4111–5

Yi F, Zhang AY, Janscha JL, Li PL, Zou AP (2004) Homocysteine activates NADH/NADPH oxidase through ceramide-stimulated Rac GTPase activity in rat mesangial cells. *Kidney Int* 66:1977–87

Zhang DX, Zou AP, Li PL (2003) Ceramide-induced activation of NADPH oxidase and endothelial dysfunction in small coronary arteries. *Am J Physiol Heart Circ Physiol* 284:H605–12

Zorov DB, Filburn CR, Klotz LO, Zweier JL, Sollott SJ (2000) Reactive oxygen species (ROS)-induced ROS release: a new phenomenon accompanying induction of the mitochondrial permeability transition in cardiac myocytes. *J Exp Med* 192:1001–14